CHEMICAL TECHNOLOGIES, MATERIALS SCIENCES, METALLURGY
ХИМИЧЕСКИЕ ТЕХНОЛОГИИ, НАУКИ О МАТЕРИАЛАХ, МЕТАЛЛУРГИЯ

UDC 621.762: 621.7 016.2
https://doi.org/10.23947/2541-9129-2025-9-3-230-241

Original Empirical Research

Influence of the Production Method and the Structure of Chromium-Nickel Corrosion Resistant Steels on the Kinetics of the Formation of the Outer Cage of Spherical Joints

EDN: OHKNMX

Nikolai A. Konko ✉, **Badrudin G. Gasanov**
Platov South-Russian State Polytechnic University (NPI), Novocherkassk, Russian Federation
✉ konko2013@mail.ru

Abstract

Introduction. Investigating the issues of wear resistance of joints, the authors of this paper have previously studied how the features of chromium-nickel corrosion resistant steels affect the shaping of the outer cage of spherical hinges. They sintered compacts made of 12Kh18N10T, VP 304.200.30 and 304L-AW-100 at 1,200°C in vacuum for 3 hours. However, in practice, it is necessary to test different steels in different conditions. This paper describes 10Kh18N9 rolled stainless steel. Powder VP 304.200.30 was sintered at 1,150°C for 2 hours. The aim of the research is to demonstrate how the production method and the metal structure affect the kinetics of the outer cage formation and, consequently, the strength of the product.

Materials and Methods. Samples made of 10Kh18N9[1] and VP 304.200.30 were radially compressed according to GOST 26529–85[2] and stretched[3] on an UMM-5[4] testing machine. Hardness was measured using a Rockwell TP 5006[5] instrument, and microhardness was measured according to Vickers on an HVS-1000[6] instrument. X-ray phase analysis was performed on an XRD-6100 diffractometer. Microscopes *Tescan VEGA* II *LMU* (for electron probe studies), *Quanta* 200 and *Altami MET*-1*M* (for studying microstructure and metallography) were used. Cold stamping of the outer cage with a spherical hinge flange was modeled in *QForm*.

Results. The strength and yield strength of VP 304.200.30 were comparable to those of some chromium-nickel austenitic steels, but were inferior in terms of ductility. A comparison between 10Kh18N9 and VP 304.200.30 revealed differences in their deformation mechanisms. The critical limitation for powder steel was not the oxide phase, but the localization of oxides at particle boundaries, which provoked brittle fracture under tension. Due to the chemical heterogeneity in the particles and residual porosity, powder steel had a 6-fold lower elongation compared to rolled steel. However, under compression conditions, sintered material could reach a hardness of 195 HV, making it suitable for use in the outer cage of spherical hinges.

Discussion. An analysis of the deformation characteristics of sintered and rolled steels confirmed the suitability of the proposed methodolo gy for assessing the deformation state of samples during cold stamping of the outer cage of spherical hinges.

Conclusion. The findings from this study allow us to predict the locations of macrodefects and optimize the manufacturing process for spherical hinges.

[1] GOST 5632–2014. *Stainless Steels and Corrosion Resisting, Heat-Resisting and Creep Resisting Alloys. Grades.* Electronic Fund of Legal and Regulatory and Technical Documents. (In Russ.) URL: https://docs.cntd.ru/document/1200113778 (accessed: 21.06.2025).
[2] GOST 26529–85. *Powder Materials. Radial Crushing Test Method.* Electronic Fund of Legal and Regulatory and Technical Documents. (In Russ.) URL: https://docs.cntd.ru/document/1200011117 (accessed: 21.06.2025).
[3] GOST 1497–84. *Metals. Methods of Tension Test.* Electronic Fund of Legal and Regulatory and Technical Documents. (In Russ.) URL: https://docs.cntd.ru/document/1200004888 (accessed: 21.06.2025).
[4] GOST 28840–90. *Machines for Tension, Compression and Bending Testing of Materials. General Technical Requirements.* Electronic Fund of Legal and Regulatory and Technical Documents. (In Russ.) URL: https://docs.cntd.ru/document/1200023577 (accessed: 21.06.2025).
[5] GOST 9013-59. *Metals. Method of Measuring Rockwell Hardness.* Electronic Fund of Legal and Regulatory and Technical Documents. (In Russ.) URL: https://docs.cntd.ru/document/1200004663 (accessed: 21.06.2025).
[6] GOST 9450–76. *Measurements Microhardness by Diamond Instruments Indentation.* Electronic Fund of Legal and Regulatory and Technical Documents. (In Russ.) URL: https://docs.cntd.ru/document/1200012869 (accessed: 21.06.2025).

Keywords: 10Kh18N9 rolled steel, VP 304.200.30 powder steel, outer race of spherical joint, microcracks in chromium-nickel steel

Acknowledgements. The authors would like to thank the Editorial board and the reviewers for their attentive attitude to the article and for the specified comments that improved the quality of the article.

For citation. Konko NA, Gasanov BG. Influence of the Production Method and the Structure of Chromium-Nickel Corrosion Resistant Steels on the Kinetics of the Formation of the Outer Cage of Spherical Joints. *Safety of Technogenic and Natural Systems*. 2025;9(3):230–241. https://doi.org/10.23947/2541-9129-2025-9-3-230-241

Оригинальное эмпирическое исследование

Влияние способа получения и структуры хромоникелевых коррозионностойких сталей на кинетику формования наружной обоймы сферических шарниров

Н.А. Конько ✉, **Б.Г. Гасанов**
Южно-Российский государственный политехнический университет (НПИ) имени М.И. Платова,
г. Новочеркасск, Российская Федерация
✉ konko2013@mail.ru

Аннотация

Введение. Исследуя вопросы износостойкости шарниров, авторы представленной работы ранее выяснили, как особенности хромоникелевых коррозионно-стойких сталей влияют на формование наружной обоймы сферических шарниров. Прессовки из 12Х18Н10Т, ВП 304.200.30 и 304L-AW-100 спекали 3 ч в вакууме при 1 200 °С. Однако практика требует испытаний разных сталей при разных условиях. В данной статье описана катаная нержавеющая сталь 10Х18Н9. Порошковую ВП 304.200.30 спекали 2 ч при 1 150 ºС. Цель работы — показать, как способ получения и структура металла определяют кинетику формования наружной обоймы сферических шарниров и в итоге — прочность изделия.

Материалы и методы. Образцы из 10Х18Н9 и ВП 304.200.30 радиально сжимали по ГОСТ 26529–85, растягивали на испытательной машине УММ-5. Твердость измеряли на приборе Роквелла ТР 5006, микротвердость — по Виккерсу на приборе HVS-1000. Рентгенофазовый анализ проводили на дифрактометре XRD-6100. Использовали микроскопы *Tescan VEGA* II *LMU* (для электронно-зондовых исследований), *Quanta* 200 и *Altami MET*-1*M* (для изучения микроструктуры и металлографии). Холодную штамповку наружной обоймы с фланцем сферического шарнира моделировали в *QForm.*

Результаты исследования. Предел прочности и текучести ВП 304.200.30 соизмерим с показателями некоторых хромоникелевых аустенитных сталей, но уступает им по пластичности. Сопоставление 10Х18Н9 и ВП 304.200.30 выявило различия в механизмах деформации. Критическое ограничение для порошковой стали — не оксидная фаза, а локализация оксидов на границах частиц, что провоцирует хрупкое разрушение при растяжении. Из-за химической неоднородности частиц и остаточной пористости относительное удлинение порошковой стали в 6 раз меньше, чем катаной. Но в условиях сжатия спеченный материал упрочняется до 195 HV, то есть подходит для производства наружной обоймы сферических шарниров.

Обсуждение. Анализ особенностей деформаций спеченных и катаных сталей подтвердил адекватность предложенной методики оценки деформированного состояния образцов при холодной штамповке наружной обоймы сферических шарниров.

Заключение. Результаты исследования позволяют прогнозировать очаги зарождения макродефектов и оптимизировать производство сферических шарниров.

Ключевые слова: катаная сталь 10Х18Н9, порошковая сталь ВП 304.200.30, наружная обойма сферического шарнира, микротрещины хромоникелевой стали

Благодарности. Авторы выражают благодарность редакции и рецензентам за внимательное отношение к статье и замечания, которые позволили повысить ее качество.

Для цитирования. Конько Н.А., Гасанов Б.Г. Влияние способа получения и структуры хромоникелевых коррозионностойких сталей на кинетику формования наружной обоймы сферических шарниров. *Безопасность техногенных и природных систем.* 2025;9(3):230–241. https://doi.org/10.23947/2541-9129-2025-9-3-230-241

Introduction. Due to the economic and technical significance of the task of extending the operational lifespan of hinge joints, which are components of many machines and mechanisms, it is essential to continuously research materials and manufacturing techniques. For instance, spherical hinge joints, which effectively absorb shock loads, are widely employed in vehicle suspensions [1]. At the same time, they are made of chromium-nickel corrosion-resistant steels, which have low wear resistance [2]. The choice of this metal for manufacturing spherical hinge parts is based on its performance characteristics during prolonged contact with aggressive media (salt solutions, moisture, and wear products). Powder metallurgy methods [4] are used to improve the tribotechnical properties of friction units made of chromium-nickel steels [3]. However, the production technology depends on the chemical composition of the material [5], the operating conditions of the machinery, the design of the friction units, and other factors [6]. Cold stamping is one option for forming the outer cage parts of spherical hinges [7] from sintered cylindrical blanks, with the inner surface coated with a solid lubricant [8] (Fig. 1).

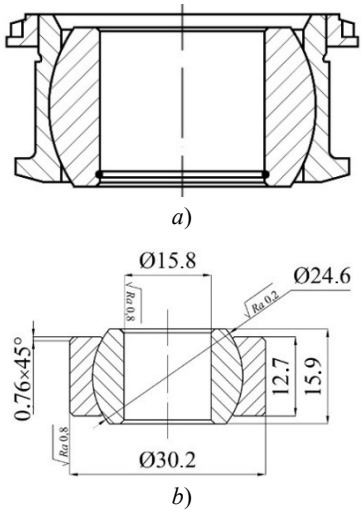

Fig. 1. The design of spherical hinge assemblies: *a* — outer cage with flange; *b* — outer cage without flange [1]

There is currently no publicly available information regarding the manufacturing process for the outer cage of spherical hinges made of sintered, corrosion-resistant steel and the estimated lifespan of these components. This has been confirmed through an analysis of recent Russian scientific literature and patents. Therefore, the following tasks are relevant:

– ensuring the required properties and quality of spherical hinges [9];

– reduction of the production costs;

– improvement of the reliability of tooling and technological equipment [10].

The team of authors of this article has already conducted scientific research in this area. Experiments with 12Kh18N10T, 304L-AW-100 and VP 304.200.30 powder steels have been described in [11]. Compacts were sintered for 3 hours in vacuum at 1,200°C. However, this is not enough. Production and operational practices are much more complex. Therefore, it is necessary to test different corrosion-resistant steels under various conditions. In this context, the following are considered:

– rolled corrosion-resistant chromium-nickel steel 10Kh18N9;

– powder steel VP 304.200.30, which was sintered for 2 hours at 1,150°C.

The aim of this research is to investigate how the production method and structure of 10Kh18N9 and VP 304.200.30 influence the kinetics of forming the outer cage of spherical hinges. The development of this approach, both theoretically and practically, opens up the potential to use data on the production method of chromium-nickel steel blanks to predict their structural formation, as well as their technological, tribological, and mechanical properties of the outer cage of spherical hinges.

Materials and Methods. Previously, studies have been conducted using corrosion-resistant chromium-nickel powder steels, such as VP 304.200.30, 304L-AW-100, and 12Kh18N10T [11]. This study focuses on the comparative analysis of VP 304.200.30 powder steel manufactured by Severstal (Russia) and its counterpart, 10Kh18N9 steel. The comparison is expected to establish a correlation between the production technology and the physical, mechanical, and operational properties of the samples.

Ring samples were made of 10Kh18N9 rolled steel (GOST 5632–2014[7]) and powder corrosion-resistant chromium-nickel VP 304.200.30 steel [11]. Geometric dimensions of the ring samples, mm:

– outer diameter of the sleeve ($D_н$) — 25;

– inner diameter of the sleeve ($d_в$) — 19.5;

– height of the sleeve (H) — 15.

The samples were obtained through the machining of 10Kh18N9 round rolled products and the static cold pressing of VP 304.200.30 powder using an HPM-60L hydraulic press in a cylindrical mold [11]. The compacting pressure varied in the range of 600–800 MPa. Powder molds were sintered in a VSl-16-22-U vacuum electric furnace at a temperature of 1150°C for two hours. The porosity of the blanks after sintering was 14–22%. Prior to cold stamping, solid lubricants were applied to the inner surface of the cylindrical sleeve: molybdenum disulfide (MoS_2) (TU 48–19–133–90[8]), pencil graphite (GOST 23463–79[9]) and polytetrafluoroethylene (PTFE, GOST 10007–80[10]) [11].

To assess the critical values of deformations during cold stamping, the ring samples, turned out of the rod and sintered, were tested for radial compression (Fig. 2) according to the procedure described in GOST 26529–85[11].

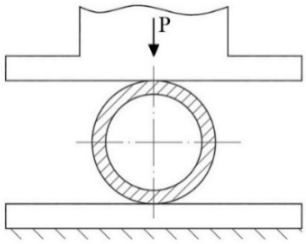

Fig. 2. Schematic of the ring sample testing for radial compression

According to the procedure described in GOST 1497–84[12], prismatic samples were produced for stretching experiments on the universal testing machine UMM-5 (GOST 28840–90[13]).

A Rockwell instrument TR 5006 (GOST 9013–59[14]) was used to determine the hardness of the samples. The microhardness was measured using the Vickers method (GOST 9450–76[15]) on an *HVS-1000* device.

The microstructure was studied using an *Altami MET-1M* metallographic microscope and a *Quanta* 200 scanning electron microscope. Electron probe surveys were performed using a *Tescan VEGA* II *LMU* scanning electron microscope. X-ray phase analysis was performed on an XRD-6100 X-ray diffractometer with a θ-2θ vertical goniometer.

The origin and development of cracks is caused by exceeding the deformation limits [12], therefore, its value during cold stamping of powder blanks is critically important and requires control at each stage of shaping [13]. Specialized software [14], calculation schemes, and simulation modeling in the *QForm* program were used to analyze the deformed state of products.

Results. The deformed state of the material of the ring samples affected their hardness after radial deformation (ε_R). To assess the relative degree of deformation, hardness was measured using the Vickers method in different sections of the ring samples (Fig. 3 *a*).

[7] GOST 5632–2014. *Stainless Steels and Corrosion Resisting, Heat-Resisting and Creep Resisting Alloys. Grades.* Electronic Fund of Legal and Regulatory and Technical Documents. (In Russ.) URL: https://docs.cntd.ru/document/1200113778?ysclid=mdohk7rxu9621196527 (accessed: 21.06.2025).

[8] TU 48–19–133–90. *Molybdenum Disulfide. Technical Specifications.* (In Russ.) URL: https://gostrf.com/normadata/1/4293788/4293788422.pdf (accessed: 21.06.2025).

[9] GOST 23463–79. *High-Purity Powdery Graphite. Specifications.* Electronic Fund of Legal and Regulatory and Technical Documents. (In Russ.) URL: https://docs.cntd.ru/document/1200014916 (accessed: 21.06.2025).

[10] GOST 10007–80. *Polytetrafluoroethylene. Specifications.* Electronic Fund of Legal and Regulatory and Technical Documents. (In Russ.) URL: https://docs.cntd.ru/document/1200020654 (accessed: 21.06.2025).

[11] GOST 26529–85. *Powder Materials. Radial Crushing Test Method.* Electronic Fund of Legal and Regulatory and Technical Documents. (In Russ.) URL: https://docs.cntd.ru/document/1200011117?ysclid=mdoi2gfjlh811854453 (accessed: 21.06.2025).

[12] GOST 1497–84. *Metals. Methods of Tension Test.* Electronic Fund of Legal and Regulatory and Technical Documents. (In Russ.) URL: https://docs.cntd.ru/document/1200004888 (accessed: 21.06.2025).

[13] GOST 28840–90. *Machines for Tension, Compression and Bending Testing of Materials. General Technical Requirements.* Electronic Fund of Legal and Regulatory and Technical Documents. (In Russ.) URL: https://docs.cntd.ru/document/1200023577 (accessed: 21.06.2025).

[14] GOST 9013–59. *Metals. Method of Measuring Rockwell Hardness.* Electronic Fund of Legal and Regulatory and Technical Documents. (In Russ.) URL: https://docs.cntd.ru/document/1200004663?ysclid=mdpkjnihrw605168957 (accessed: 21.06.2025).

[15] GOST 9450–76. *Measurements Microhardness by Diamond Instruments Indentation.* Electronic Fund of Legal and Regulatory and Technical Documents. (In Russ.) URL: https://docs.cntd.ru/document/1200012869?ysclid=mdpkn680t1373636400 (accessed: 21.06.2025).

a) *b*)

Fig. 3. Radial upsetting of annular samples:
a — 10Kh18N9 rolled steel; *b* — simulation of radial upsetting from dispersed VP 304.200.30 powder

The hardness in different zones of the ring samples differed significantly. For example, in tension zones 1 and 2 for ring samples made of 10Kh18N9 steel, the hardness varied from 190 HV to 205 HV. The indicator for VP 304.200.30 sintered steel was 130–140 HV. In compression zones 3 and 4, the hardness was slightly higher: 210–230 HV for 10Kh18N9 and 185–195 HV for VP 304.200.30.

This could be explained by the fact that the stress-strain state of the material depended on the configuration of the workpieces before and after radial upsetting. In zone A (3 and 4), the material strengthened better as a result of plastic deformation (work hardening) than in tension zones B (1 and 2) (Fig. 3 *b*).

It is known from [11] that when upsetting sintered ring samples with an austenitic structure and porosity of 18–20% (Fig. 4 *a*), cracks appear at the interparticle boundaries with increased concentrations of Cr_2O_3, CrO_2 (Fig. 4 *b*). The analysis of the results from mapping the crack mouth showed that microcracks were developing:

– along interparticle boundaries with a higher concentration of O;

– in areas with heterogeneous chemical composition (Fig. 4 *c*).

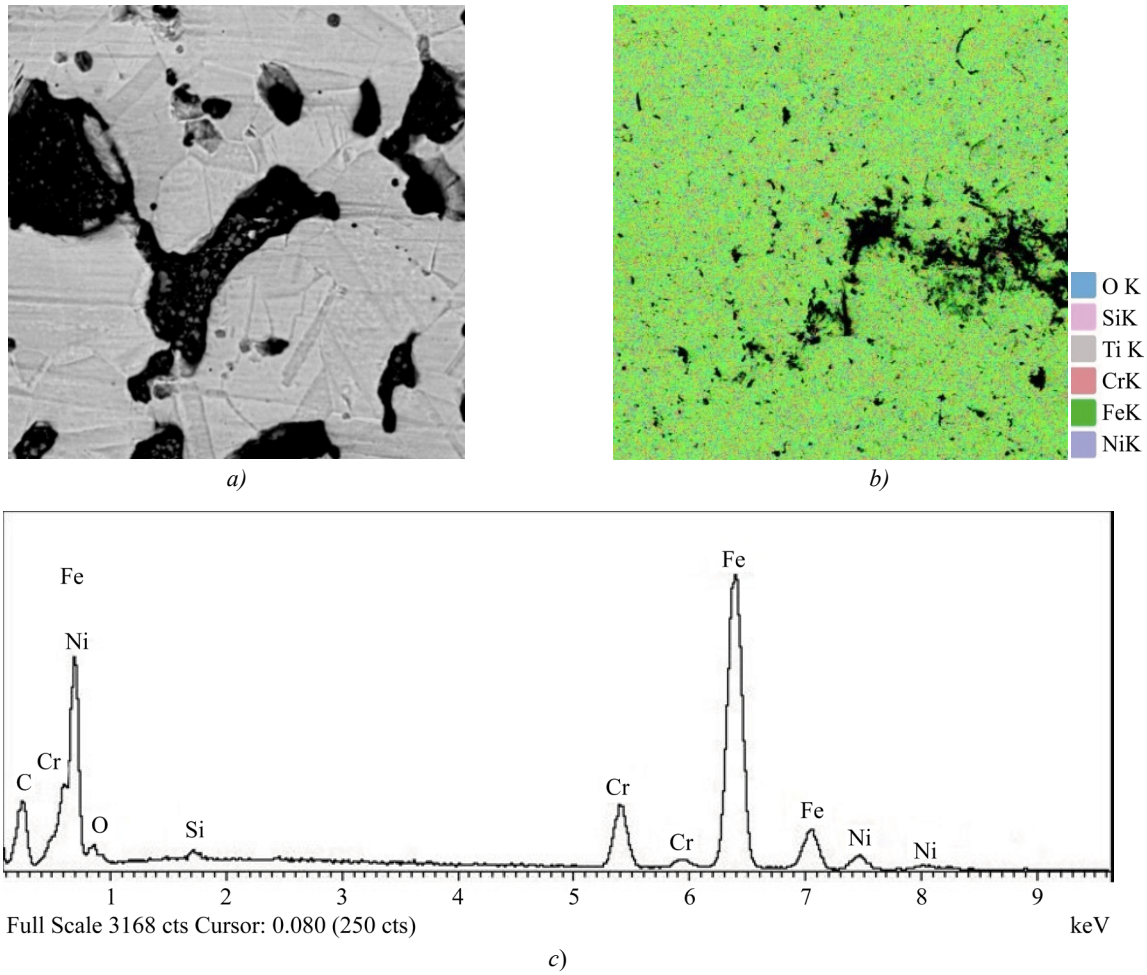

a) *b*)

c)

Fig. 4. Mapping of a sintered ring sample made of VP powder 304.200.30 (Si — 0.7, Cr — 12.2, Fe — 75.5, Ni — 7.90, O — 3.7):
a — microstructure before testing; *b, c* — distribution of chemical elements in the crack mouth after radial deformation

Plastic properties of sintered steels were particularly strongly influenced by the distribution of chromium oxides and carbides in areas of intense plastic deformation. This was confirmed by the mapping of microsection sites at the crack mouth (Fig. 5).

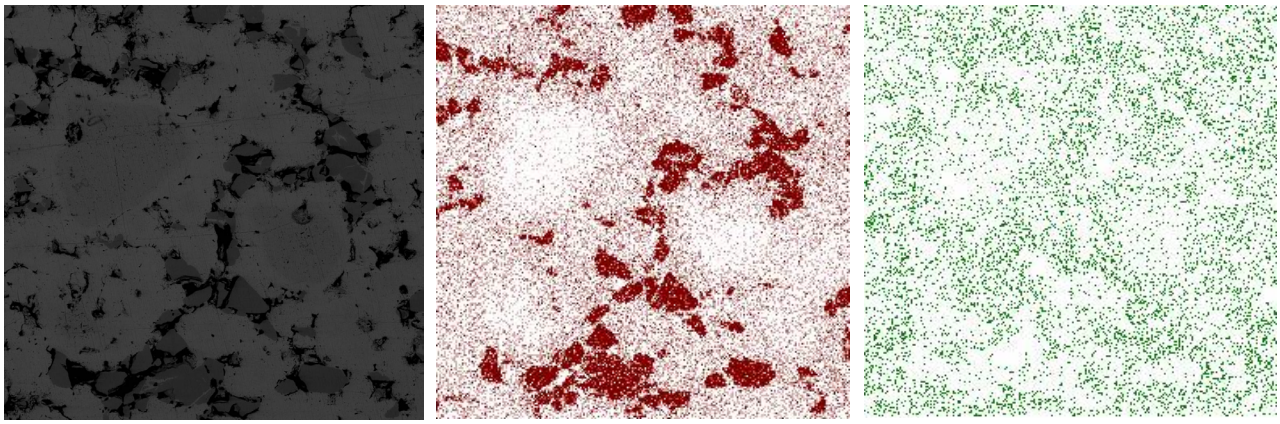

a) *b)* *c)*

Fig. 5. Mapping of sintered VP 304.200.30 chromium-nickel steel:
a — microstructure; *b, c* — distribution of Cr and Ni

In the 10Kh18N9 rolled steel samples, the steel structure was more homogeneous in chromium and nickel (Fig. 6 *a*). The content of foreign inclusions was significantly less than in sintered steel from dispersed powders with similar compositions (Fig. 6 *b, c*).

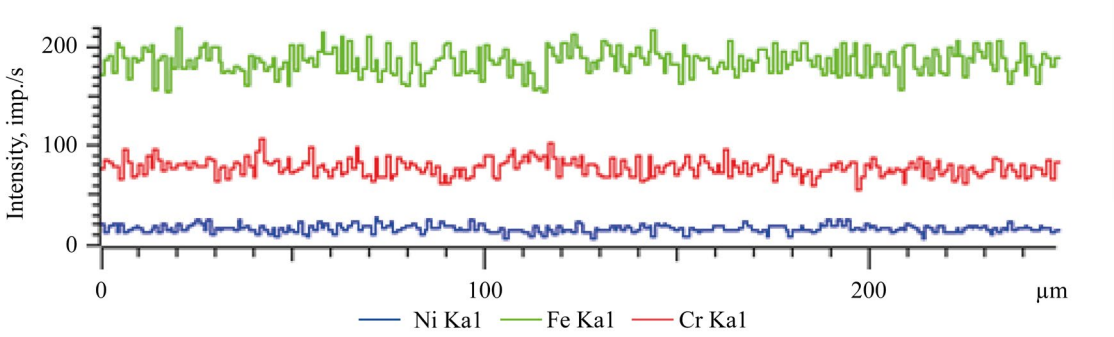

a)

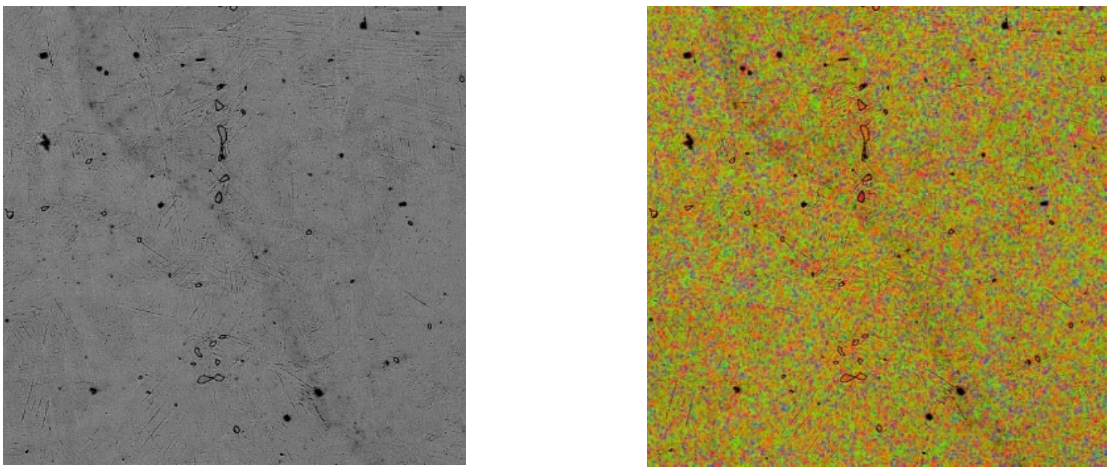

b) *c*)

Fig. 6. Mapping of 10Kh18N9 steel:
a — distribution of Cr and Ni; *b, c* — microstructure

When ring samples were upset, the shear deformation of the material was provided by various mechanisms. Their contribution was determined by the scheme and degree, size, grain shape and porosity of the workpieces before deformation, chemical and phase composition of the material (Fig. 7 *a*), properties and size of excess phases and other conditions.

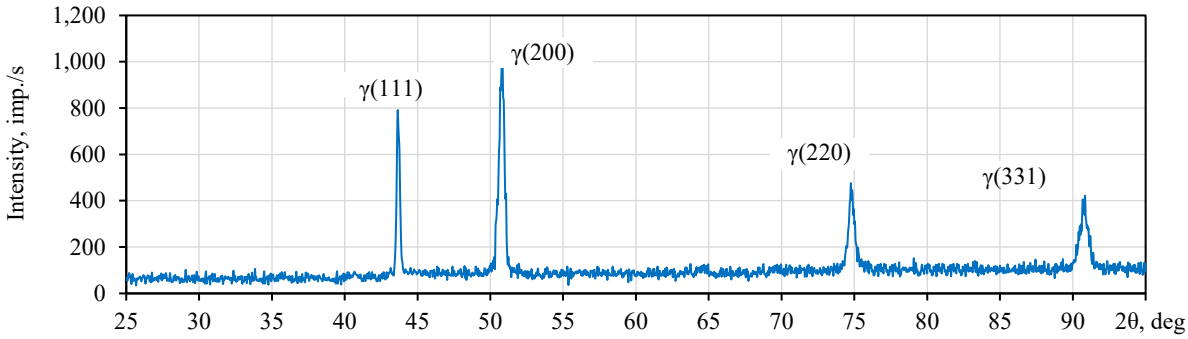

a)

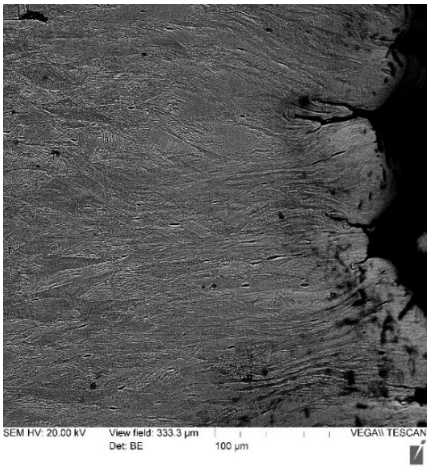

b)

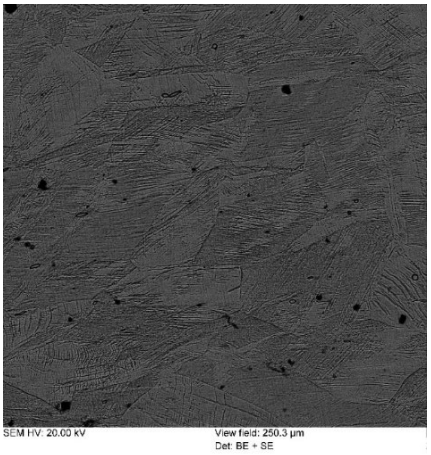

c)

Fig. 7. Phase analysis and microstructure of 10Kh18N9 rolled steel:
a — diffractogram after radial compression; *b* — microstructure of rings in the compression zone;
c — microstructure in the stretching zone after upsetting ε_R = 63 %

Therefore, lineage structure in certain sections, characteristic of rolled chromium-nickel steels of the austenitic class (Fig. 7 *a*), not only reduced their plastic properties, but also affected the kinetics of microstructure formation after cold stamping. Inhomogeneous deformation in different parts of the sample was the cause of twinning, deformation bands, and transition bands (Fig. 7 *b, c*).

The mechanical properties of sintered blanks made of VP 304.200.30 chromium-nickel steel powders were influenced by several factors:

– the initial microstructure and the presence of foreign inclusions;

– the microstructure and chemical composition of the particles formed during the melt sputtering and cooling of the powder particles.

Apparently, upon rapid cooling, stable α-phase nuclei with an increased concentration of iron were formed in liquid melt droplets (Fig. 8 *a*). In particular, such spherical particles (Table 1, Fig. 8, Spectrum 3) contained about 91% (at.) of iron, while nuclei of other particles (Table 1, Fig. 8, Spectrum 2) contained about 80%. In other areas of the same particles, the Cr content reached 74% (at., Table 1, Fig. 8, Spectrum 1). This was several times higher than its average concentration in steel powders. In this case, the word “spectrum” refers to the place and order of spike on the examined microsection.

Table 1

Distribution of chemical elements in sintered steel of VP 304.200.30 powder
on various sections of particles in samples before cold stamping

Spectrum	Si	Cr	Mn	Fe	Ni	Total
1	0.07	74.63	0.70	24.29	0.31	100
2	2.24	10.25	0.31	80.22	6.99	100
3	1.03	6.12	0.09	91.28	1.49	100

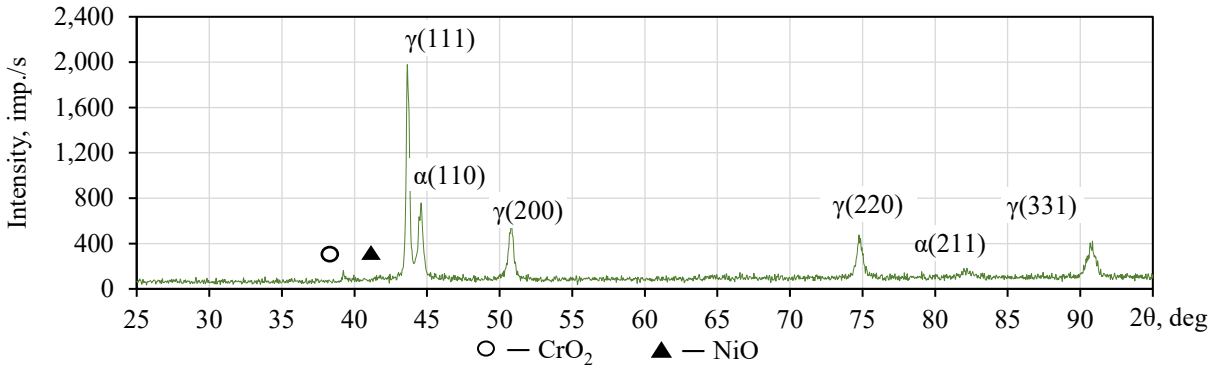

a)

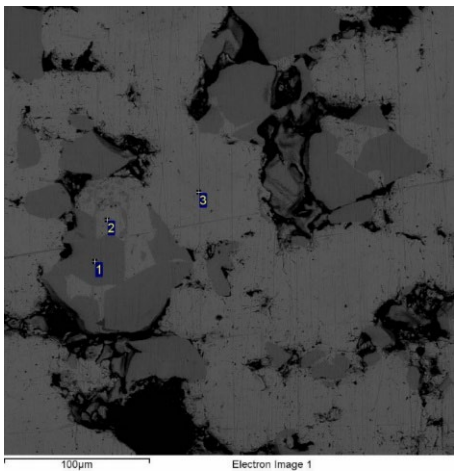

b)

Fig. 8. Phase composition and microstructure of samples before cold stamping in sintered steel of VP powder 304.200.30:
a — diffractogram; *b* — distribution of chromium, nickel and other elements

During sintering of the samples from dispersed VP 304.200.30 powder at a temperature of 1150–1180°C for 2 hours, diffusion homogenization occured. Chromium, nickel, and iron were mutually dissolved and distributed more evenly over the volume (Fig. 9), which generally affected the ductility of the blanks sintered in vacuum.

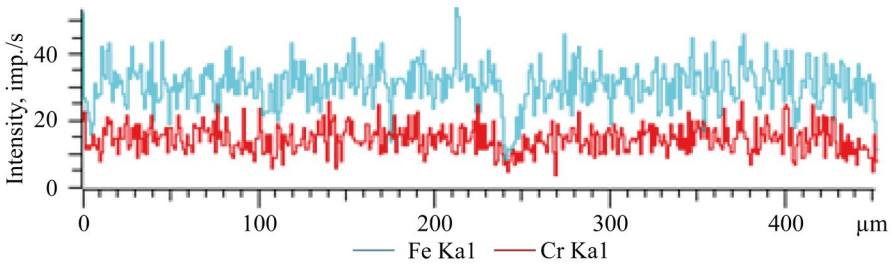

a)

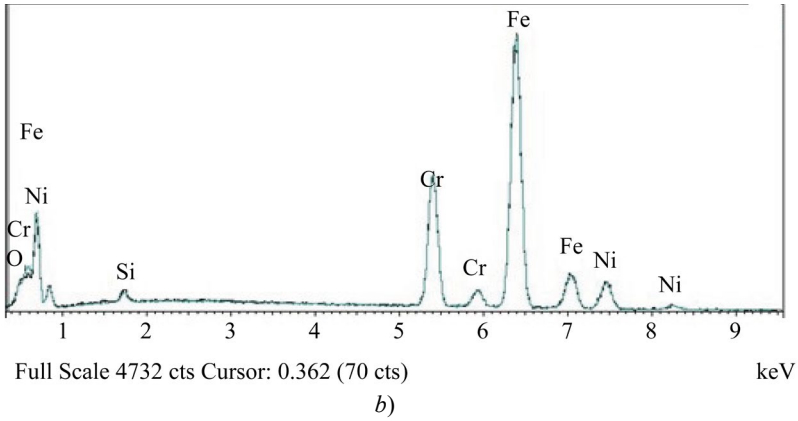

b)

Fig. 9. Distribution of chemical elements in sintered steel of VP 304.200.30 powder:
a — linear distribution of Cr and Fe; *b* — spectral analysis of Cr, Ni and other elements

The larger the pore in the interparticle boundaries, the greater the difference in particle deformation, especially with small medium deformations of the material. Therefore, the microstructure of sintered steel after upsetting and, consequently, the microhardness differed markedly in different areas of the same zone (Fig. 10).

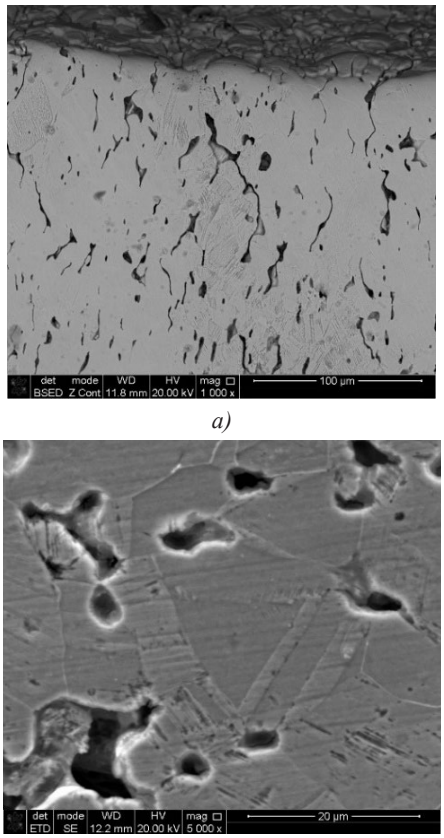

a)

b)

Fig. 10. Microstructure of sintered VP 304.200.30 steel:
a — compression zone (A); *b* — stretching zone (B) after upsetting $\varepsilon_R \approx 0.5$

The tensile strength of vacuum-sintered steels made of VP 304.200.30 powder was comparable to the strength and yield strength of some austenitic chromium-nickel steels, but inferior to them in terms of ductility (Table 2).

Table 2

Physical-mechanical properties of chromium-nickel corrosion-resistant steels

Material	Properties					
	σ_s, MPa	δ, %	Ψ, %	Π, %	ρ, g/cubic cm	Hardness
10Kh18N9	195.00	45.00	55.00	–	7.90	29 HRC
VP 304.200.30	180.63	7.67	8.08	19.05	6.65	45 HRB

Thus, an analysis of the fracture mechanism during upsetting of rings made of stainless chromium-nickel steels revealed that the strength and ductility of sintered steel in the tensile zone depended not only on the stress-strain state of the material. In this case, two more factors were important:

– the quality of the contact between the particles;

– the presence of foreign inclusions on the surface of the dispersed powders.

Modeling of the cold stamping process of an outer cage with a spherical hinge flange in the *QForm* program (Fig. 11) gave an idea of the kinetics of shaping [15]. Sintered cylindrical blanks made of VP 304.200.30 powder were used. The zone highlighted in dark green had a minimum plasticity resource. This was where macro- and micro-cracks could originate.

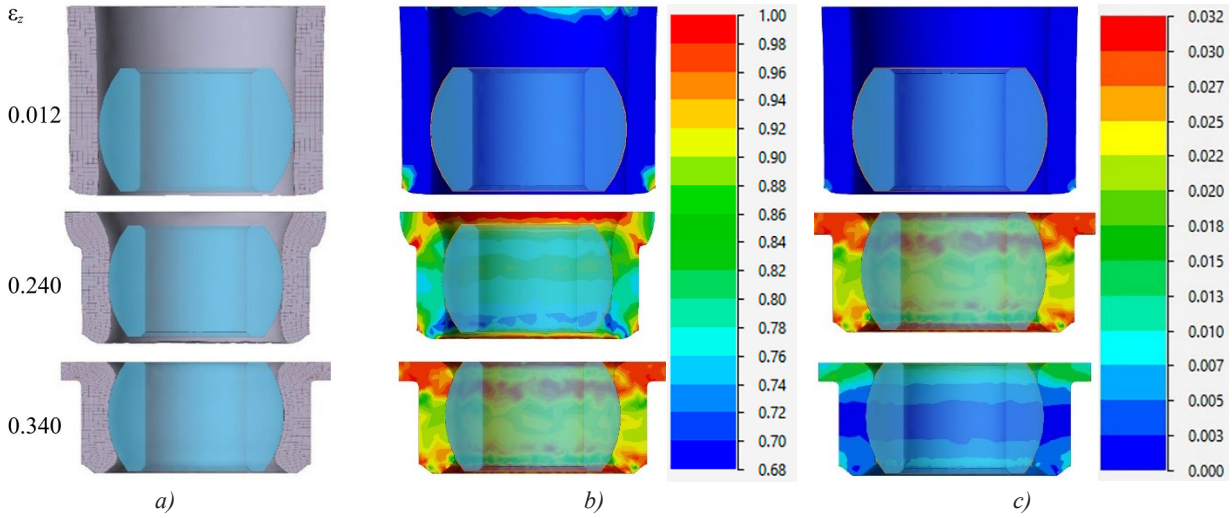

Fig. 11. Simulation modeling of the kinetics of forming an outer cage with a flange of a porous blank in the *QForm* program: *a* — change in the coordinate grid; *b* — volume distribution of relative density; *c* — plasticity resource

In Figure 11 ε_z is a dimensionless quantity. This is a relative degree of deformation, that is, the ratio of the absolute deformation (change in size) to the original length of the body. During the modeling process, a coordinate grid was applied to the sample, and during deformation, the material was distorted, as can be seen in Figure 11. The figure shows the direction in which the material moved during deformation.

A comparison of 10Kh18N9 rolled steel and VP 304.200.30 powder steel revealed fundamental differences in the deformation mechanisms. For powder steel, the critical limitation was not the oxide phase, but the localization of oxides at the particle boundaries, which provoked brittle fracture under tension. The chemical heterogeneity of the particles and the residual porosity exacerbated the problem: in comparison with rolled steel, the elongation decreased by 6 times (see the indicator δ in Table 2). At the same time, under compression conditions, the sintered material hardened to 195 HV, and this indicated the possibility of its use in the manufacture of external spherical hinges.

Discussion. To conclude, during the deformation of sintered workpieces, the intensity of stress fields in the contact zones of powder particles and on the pore surfaces differed significantly from the average values. According to [11], the critical value of the strain intensity during radial upsetting of ring samples made of VP 304.200.30 powder was 0.195. This caused inhomogeneity of deformations, and also prevented the determination of the deformed state by the plasticity condition (if the stress state is known). The patterns of the main deformations determined the uneven and anisotropic nature of changes in the mechanical properties of the sintered parts during cold stamping. Therefore, the plasticity resource was affected not only by the porosity, but also by the deformed state of the material. This has been confirmed experimentally.

The analysis of the deformation behavior of sintered and rolled steels, as described in the article, confirmed the validity of the proposed method for assessing the deformed state of cylindrical blanks during cold stamping of the outer cages of spherical hinges. Practical application of the results from this study will enhance the efficiency of chromium-nickel steel manufacturing processes. Based on the findings of the scientific research presented in the article, it appears that this material would be an ideal choice for spherical hinges.

Conclusion. The revealed mechanism of sintered chromium-nickel steel destruction during cold stamping allows us to estimate the critical strain intensity values and the effect of steel structure on its tensile ductility in this zone.

We have established that the plasticity resource of sintered chromium-nickel stainless steels depends not only on the stress-strain state of the material, but also on the initial structure, the presence of impurities, as well as the quality of interparticle contacts and grain boundaries.

Our research focused on the qualitative features of spherical hinges used in vehicle suspensions. Experimental and simulation studies have revealed the technological aspects of their production through cold stamping of sintered workpieces.

References

1. Mikhailov AN, Matvienko SA, Strelnik YuN, Lukichev AV. Functionally-Oriented Analysis of the Operating Conditions and Production Technologies of Transport Vehicles Spherical Swivel Connections. In: *Proceedings of the International Scientific and technical conference "Technical operation of Water Transport: Problems and Ways of Development" Petropavlovsk-Kamchatsky, 17–19 October, 2018.* Petropavlovsk-Kamchatsky: Kamchatka State Technical University; 2019. P. 112–115. (In Russ.)

2. Haidorov AD, Yunusov FA. Vacuum Heat Treatment of high Alloy Corrosion-Resistant Steels. *St. Petersburg Polytechnic University Journal of Engineering Sciences and Technology.* 2017;23(1):226–235. (In Russ.) http://doi.org/10.18721/JEST.230123

3. Woodhead J, Truman CE, Booker JD. Modelling of Dynamic Friction in the Cold Forming of Plain Spherical Bearings. *Surface and Contact Mechanics Including Tribology XII*. 2015;91:141–152. http://doi.org/10.2495/SECM150131

4. Ilyuschenko AF. Current Developments in Powder Metallurgy for Mechanical Engineering. *Mechanics of Machines, Mechanisms and Materials.* 2012;(3(20)–4(21)):113–120. (In Russ.) URL: https://mmmm.by/pdf/ru/2012/3_4_2012/11.pdf (accessed: 02.06.2025).

5. Hojati M, Danninger H, Gierl-Mayer Ch. Mechanical and Physical Properties of Differently Alloyed Sintered Steels as a Function of the Sintering Temperature. *Metals*. 2022;12(1):13–20. https://doi.org/10.3390/met12010013

6. Bram M, de Freitas Daudt N, Balzer H. Porous Metals from Powder Metallurgy Techniques. *Encyclopedia of Materials: Metals and Alloys*. 2022;3:427–437. https://doi.org/10.1016/B978-0-12-819726-4.00093-4

7. Lingzhu Gong, Xiaoxiang Yang, Kaibin Kong, Shuncong Zhong. Optimal Design for Outer Rings of Self-Lubricating Spherical Plain Bearings Based on Virtual Orthogonal Experiments. *Advances in Mechanical Engineering*. 2018;10(6):1–11. https://doi.org/10.1177/1687814018783402

8. Gasanov BG, Konko NA, Baev SS. Study of the Kinetics of Forming of Spherical Sliding Bearing Parts Made of Corrosion-Resistant Steels by Die Forging of Porous Blanks. *Metal Working and Material Science.* 2024;26(2):127–142. (In Russ.) http://doi.org/10.17212/1994-6309-2024-26.2-127-142

9. Rozenberg OA, Mikhailov OV, Shtern MB. Strain Hardening of Porous Bushings by Multiple Mandreling: Numerical Simulation. *Powder Metallurgy and Metal Ceramics*. 2012;51:379–384. http://doi.org/10.1007/s11106-012-9445-y

10. Kondo H, Hegedus M. Current Trends and Challenges in the Global Aviation Industry. *Acta Metallurgica Slovaca.* 2020;26(4):141–143. https://doi.org/10.36547/ams.26.4.763

11. Gasanov BG, Konko NA, Baev SS. The Effect of the Method for Producing Chromium-Nickel Stainless Steel Powders on the Strain State and Properties of the Outer Cage of a Spherical Hinge Joint. *Diagnostics, Resource and Mechanics of Materials and Structures*. 2024;5:138–158. (In Russ.) https://doi.org/10.17804/2410-9908.2024.5.138-158

12. Kovalchenko MS. Deformation Hardening of a Powder Body during Pressing. *Powder Metallurgy.* 2009;(3/4):13–27. (In Russ.)

13. Egorov MS, Egorova RV, Pustovoit VN, Atrokhov AA. Mechanical Properties of Powder Materials after Hot Forging. *Metallurg*. 2020;3:92–96. (In Russ.)

14. Burlakov IA, Zabelyan DM, Bondarenko AK, Gladkov YuA, Leonidov AN. Efficient Utilization of the Plasticity Resource at Cold Forming of Sheet Workpieces Based on the Cockroft and Kolmogorov Criteria. *Forging and Stamping Production. Material Working by Pressure*. 2016;(12):3–8. (In Russ.)

15. Baglyuk GA, Kurikhin VS, Khomenko AI, Kozachenko IS. Improving Methods for Studying the Strain Distribution in Powders During Compaction. *Powder Metallurgy and Metal Ceramics*. 2015;54:129–135. (In Russ.) https://doi.org/10.1007/s11106-015-9689-4

About the Authors:

Nikolai A. Konko, Assistant Professor of the Department of General Engineering Disciplines, Platov South Russian State Polytechnic University (NPI) (132, Prosveshcheniya Str., Novocherkassk, 346428, Russian Federation), SPIN-code, ORCID, ResearcherID, konko2013@mail.ru

Badrudin G. Gasanov, Dr. Sci. (Eng.), Professor of the Department of International Logistics Systems and Complexes, Platov South Russian State Polytechnic University (NPI) (132, Prosveshcheniya Str., Novocherkassk, 346428, Russian Federation), SPIN-code, ORCID, ScopusID, gasanov.bg@gmail.com

Claimed Contributorship:

NA Konko: formal analysis, research, methodology, validation, visualization, writing – original draft preparation.
BG Gasanov: conceptualization, data curation, supervision.

Conflict of Interest Statement: **the authors declare no conflict of interest.**

All authors have read and approved the final manuscript.

Об авторах:

Николай Андреевич Конько, ассистент кафедры «Общеинженерные дисциплины», Южно-Российского государственного политехнического университета (НПИ) имени М.И. Платова (346428, Российская Федерация, г. Новочеркасск, ул. Просвещения, 132), SPIN-код, ORCID, ResearcherID, konko2013@mail.ru

Бадрудин Гасанович Гасанов, доктор технических наук, профессор кафедры «Международные логистические системы и комплексы» Южно-Российского государственный политехнический университет (НПИ) имени М.И. Платова (346428, Российская Федерация, г. Новочеркасск, ул. Просвещения, 132), SPIN-код, ORCID, ScopusID, gasanov.bg@gmail.com

Заявленный вклад авторов:

Н.А. Конько: формальный анализ, проведение исследования, разработка методологии, валидация результатов, визуализация, написание черновика рукописи.

Б.Г. Гасанов: создание концепции, курирование работы с данными, научное руководство.

Конфликт интересов: **авторы заявляют об отсутствии конфликта интересов.**

Авторы прочитали и одобрили окончательный вариант рукописи.

Received / Поступила в редакцию 30.06.2025
Reviewed / Поступила после рецензирования 14.07.2025
Accepted / Принята к публикации 25.07.2025